ORIGINAL ARTICLE

Clinical, histopathological and molecular risk factors for recurrence of pilocytic astrocytomas: brainstem/spinal location, nestin expression and gain of 7q and 19 are associated with early tumor recurrence

Ryota Tamura[1] · Akio Iwanami[2,4,5] · Kentaro Ohara[3] · Masaaki Nishimoto[1] · Eriel Sandika Pareira[1] · Tomoru Miwa[1] · Naoko Tsuzaki[1] · Yuki Kuranari[1] · Yukina Morimoto[1] · Masahiro Toda[1] · Hideyuki Okano[3] · Masaya Nakamura[2] · Kazunari Yoshida[1] · Hikaru Sasaki[1,6]

Abstract

Pilocytic astrocytomas (PAs) are benign tumors. However, clinically aggressive PAs despite benign histology have been reported, and histological and molecular risk factors for prognosis have not been elucidated. 38 PAs were studied for clinical, histological, and molecular factors, including tumor location, extent of resection, post-operative treatment, glioma-associated molecules (IDH1/2, ATRX, BRAF, FGFR1, PIK3CA, H3F3A, p53, VEGF, Nestin, PD-1/PD-L1), CDKN2A/B deletion, and chromosomal number aberrations, to see if there is any correlation with patient's progression-free survival (PFS). Brainstem/spinal location, extent of resection and post-operative treatment, and VEGF-A, Nestin and PD-L1 expression, copy number gain of chromosome 7q or 19, TP53 mutation were significantly associated with shorter PFS. None of the histological parameters was associated with PFS. Multivariate analyses demonstrated that high Nestin expression, gain of 7q or 19, and extent of removal were independently predictive for early tumor recurrence. The brainstem/spinal PAs appeared distinct from those in the other sites in terms of molecular characteristics. Clinically aggressive PAs despite benign histology exhibited high Nestin expression. Brainstem/spinal location, extent of resection and some molecular factors including Nestin expression and gains of 7q and 19, rather than histological parameters, may be associated with early tumor recurrence in PAs.

✉ Hikaru Sasaki
hsasaki@keio.jp

1 Department of Neurosurgery, Keio University School of Medicine, 35 Shinanomachi, Shinjuku-Ku, Tokyo 160-8582, Japan

2 Department of Orthopaedic Surgery, Keio University School of Medicine, 35 Shinanomachi, Shinjuku-Ku, Tokyo 160-8582, Japan

3 Department of Pathology, Keio University School of Medicine, 35 Shinanomachi, Shinjuku-Ku, Tokyo 160-8582, Japan

4 Department of Physiology, Keio University School of Medicine, 35 Shinanomachi, Shinjuku-Ku, Tokyo 160-8582, Japan

5 Department of Orthopaedic Surgery, Spine Center, Koga General Hospital, 1555 Koga, Ibaraki 306-0041, Japan

6 Division of Neurosurgery, Tokyo Dental College Ichikawa General Hospital, 5-11-13, Sugano, Ichikawa, Chiba 272-8513, Japan

Abbreviations

CAN	Chromosomal number aberrations
CDKN	Cyclin dependent kinase inhibitor
FGFR	Fibroblast growth factor receptor 1
FISH	Fluorescence in situ hybridization
GTR	Gross total removal
H&E	Haematoxylin and eosin
IDH	Isocitrate dehydrogenase
MAPK	Mitogen-activating protein kinase
NF1	Neurofibromatosis type 1
OS	Overall survival
PA	Pilocytic astrocytoma
PCR	Polymerase chain reaction
PFS	Progression-free survival
PIK3CA	Phosphatidylinositol-4,5-bisphosphate 3-kinase catalytic subunit alpha
PDGFR β	Platelet-derived growth factor receptor-beta
PD-1	Programmed cell death-1
PD-L1	Programmed death-ligand 1
STR	Subtotal removal

VEGF Vascular endothelial growth factor
VHL Von Hippel-Lindau
WHO World health organization

Introduction

Pilocytic astrocytoma (PA) is a World Health Organization (WHO) grade I brain tumor with a 10-year survival rate of more than 95% [1]. PAs preferentially arise in the cerebellum, followed by the cerebrum, opticohypothalamic region, spinal cord, and brainstem, and typically occur in young adults [1]. Nearly all PAs are associated with alteration of the mitogen-activating protein kinase (MAPK) pathway, with the most common mechanism being a tandem duplication of a fragment on chromosome 7q, resulting in a KIAA1549-BRAF fusion protein [1].

A small portion of PAs is clinically aggressive despite their typical histologic features, and cases of PAs with anaplastic features are described in the literature [2]. Rodriguez et al. [2] classified PAs into 3 groups; conventional PAs, clinically aggressive PAs, and histologically anaplastic PAs, and they reported anaplastic PAs as being associated with the worst overall survival (OS). Prognostic factors in patients with PAs reported in the literature include patient age, extent of resection, prior irradiation, presence of necrosis, positive p53 staining, high-mitotic activity, and activation of the PI3K/AKT pathway [2, 3]. However, the molecular mechanism underlining clinical aggressiveness in PAs has not been fully elucidated, and the findings regarding the biological behavior of anaplastic PAs were not consistent [1]. Furthermore, the role of angiogenic factors, stemness markers, and immune checkpoint molecules, which have been found to be correlated with tumor progression and patient prognosis in several types of brain tumors [4–6], have not been well examined in PAs. In the present study, molecular factors involved in pathological classification (IDH1/2, ATRX, H3F3A) or known to be associated with glioma development and biological behavior (PIK3CA, p53, vascular endothelial growth factor [VEGF], Nestin, programmed cell death-1 [PD-1]/ programmed cell death-ligand 1 [PD-L1], cyclin dependent kinase inhibitor (CDKN) 2A/B and MAPK pathway genes such as BRAF and FGFR1) were investigated. Furthermore, the clinical, and histological prognostic factors were analyzed in association with patients' progression-free in PAs.

Methods

Tumor samples

Pathology records of brain tumors treated at Department of Neurosurgery, and Orthopaedic Surgery, Keio University

Hospital between 2014 and 2017 were reviewed. Patients with brain tumors of which institutional histological diagnosis was PA according to WHO criteria were included in the study [7, 8]. Written informed consent for the translational research was obtained from all the enrolled patients. This research has been approved by the Institutional Review Board at our institute (IRB No. 20050002).

Clinical and histological evaluation

Tumors were classified by their primary sites; cerebellum, supratentorium, brainstem, spinal cord, opticohypothalamus and aqueduct. PAs epicentered on the aqueduct have been reported as unique entity (Fig. 1A) [9, 10]. The extent of resection was determined by review of medical records. Histopathological findings were assessed by a neuropathologist (KO) using haematoxylin and eosin (H & E) based scoring system; cellularity (1:mild, 2:moderate, 3:marked), nuclear atypia (1:mild, 2:moderate, 3:marked), mitosis (0: absent, 1: present), endothelial proliferation (0:absent, 1:present) and necrosis (0: absent, 1:present) (Fig. 2A). Anaplastic PA was defined as PA with high mitotic activity, hypercellular areas with hyperchromatic, enlarged nuclei and multinuclear giant cells, with or without necrosis and endothelial proliferation, as previously described [3]. Clinically aggressive PA was defined as PA progressing despite adequate therapy or requiring additional surgical intervention within a year of surgery, but lacking histologic features of anaplasia, as previously described [2].

Immunohistochemical analysis

Standard immunohistochemistry was carried out, as previously described [11, 12]. Expression levels of Ki-67, vascular endothelial growth factor (VEGF) -A, VEGF receptor 1 (VEGFR1), VEGFR2, Nestin, PD-1, PD-L1, CD3, CD8, p53, ATRX, H3K27M, and BRAF V600E were examined via immunohistochemistry. The results of the immunohistochemical analysis were noted in Supplemental methods [11–13].

DNA extraction and metaphase comparative genomic hybridization (CGH)

DNA was extracted by microdissection of the representative area of each tumor from 4 um sections of formalin-fixed paraffin-embedded tissues. Metaphase CGH was performed as previously described (Supplemental methods) [14, 15].

Direct sequencing

Isocitrate dehydrogenase (IDH)1 codon 132, IDH2 codon 172, fibroblast growth factor receptor (FGFR)1 codon

Fig. 1 General characteristics.
A This study includes PAs located on the cerebellum (n = 14), spinal cord (n = 7), opticohypothalamus (n = 7), supratentorium (n = 6), brainstem (n = 3), and aqueduct (n = 1). **B** Kaplan–Meier curve of PFS and OS for all patients. **C** Kaplan–Meier curve of PFS according to tumor location
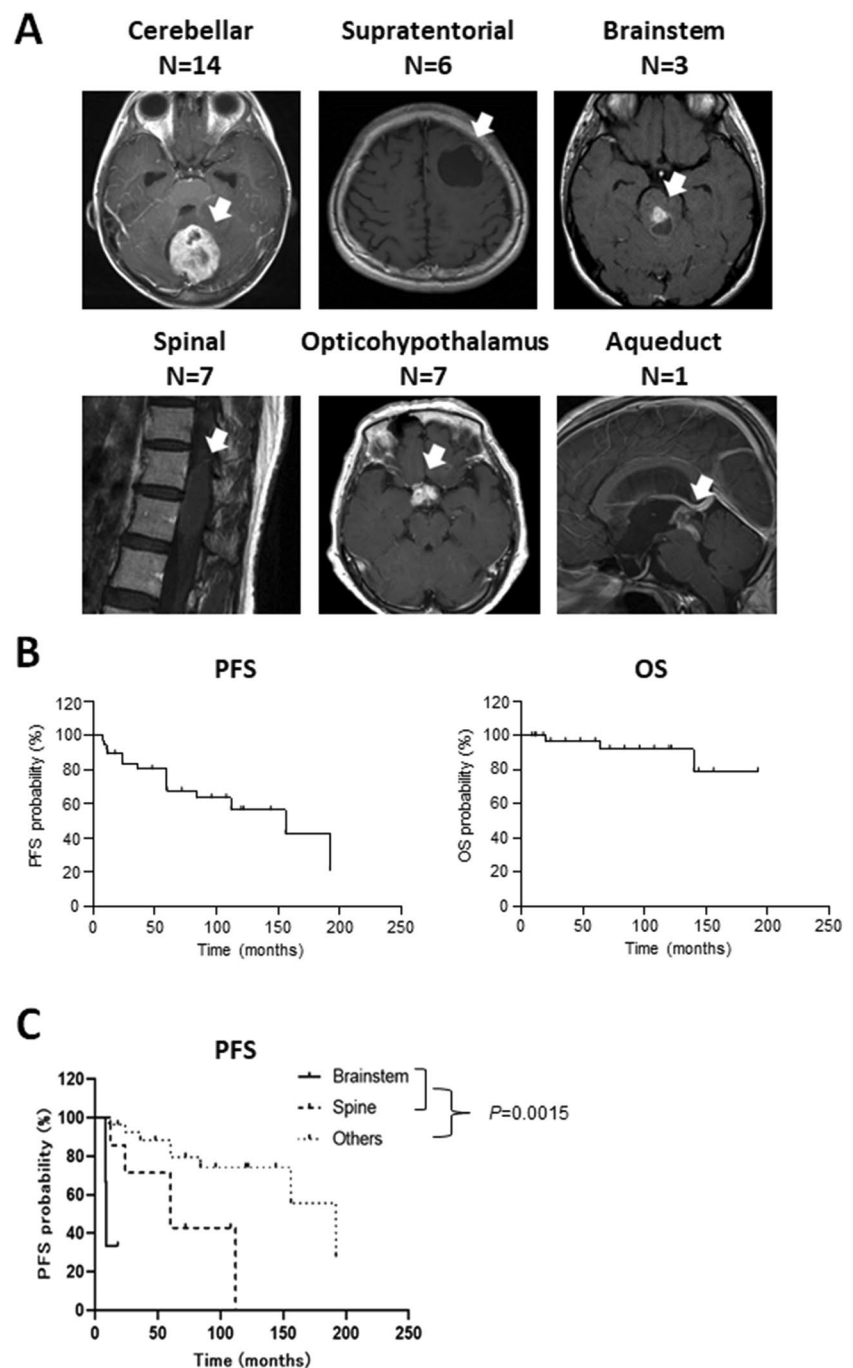

546 and 656, phosphatidylinositol-4,5-bisphosphate 3-kinase catalytic subunit alpha (PIK3CA) codon 1047, BRAF codon 600, and H3F3A codon 27 were examined by Sanger sequencing following polymerase chain reaction (PCR). Sequencing was performed using Applied Biosystems 3730xl DNA analyzer (Thermo Fisher Scientific), as previously described [16, 17]. Primer sequences are listed in Supplementary Table S1.

Fluorescence in situ hybridization (FISH)

FISH probes were generated to detect KIAA1549-BRAF fusions from the corresponding clone from a library of human genomic clones (clone no. TR015, GSP Laboratory, Inc.), which could detect the great majority of patterns of previously reported KIAA1549-BRAF fusions; detection of 16–9, 15–9 and 16–11 fusions was validated

Fig. 2 Histopathological analysis. **A** Our scoring system uses the following parameters; cellularity (1: mild, 2: moderate, 3: marked), atypia (1: mild, 2: moderate, 3: marked), mitosis (0, 1), endothelial proliferation (0,1), and necrosis (0,1). **B** Typical PAs with low and high histological scores. The low-score case shows low cellularity composed of bipolar cells with microcysts. The high-score case shows high mitotic activity, hypercellular areas with enlarged nuclei and endothelial proliferation. Scale bar, 100 μm. **C** Histopathological score for PAs per location and subsets (PA, CAP and APA). The mean (bar) and SD (error bars) are shown. **D** Ki-67-positive cell ratio for PAs per location and subset (PA, CAP, and APA). The mean (bar) and SD (error bars) are shown. *PA* conventional pilocytic astrocytoma, *CAP* clinically aggressive PA, *APA* histologically anaplastic PA
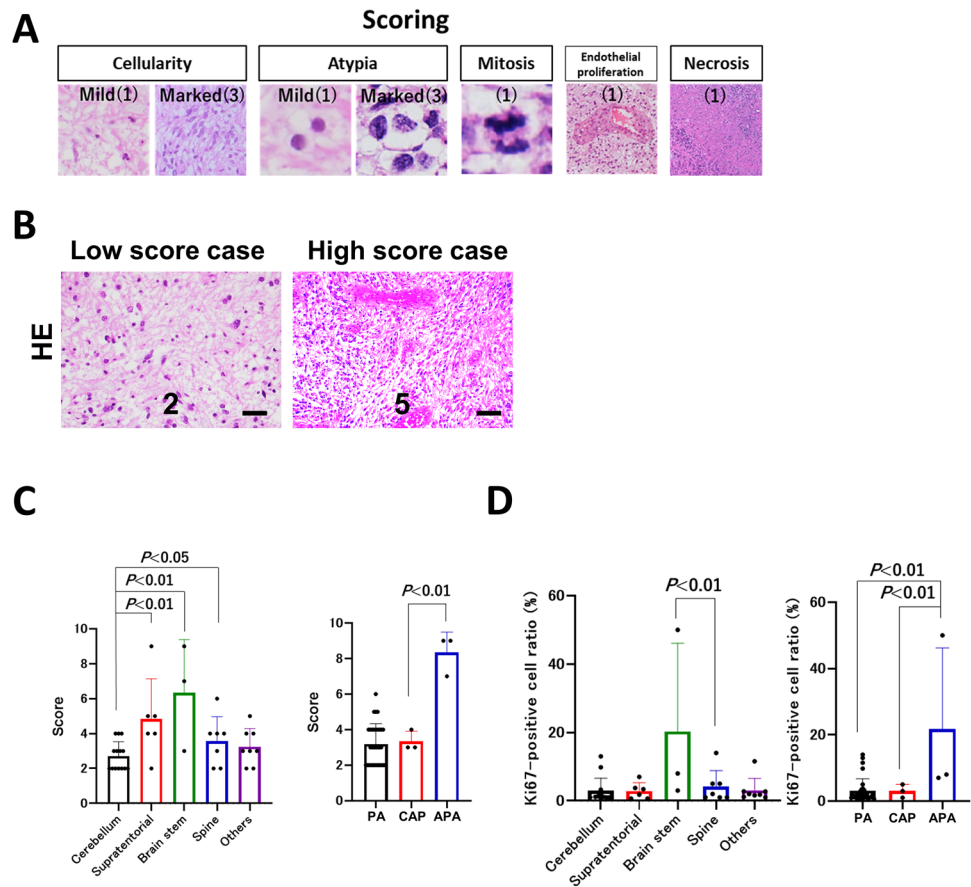
by PCR-sequencing flanking the fusions (Supplementary Fig. S1A) [18]. KIAA1549 was labeled with fluorescein isothiocyanate and BRAF with Texas Red. The probes were successfully tested on the slides with normal lymphocytes in metaphase. Fusion was confirmed by a yellow signal generated by the overlap of the KIAA1549 and BRAF signals. Sections from oligodendroglioma, IDH mutant, 1p/19q codeleted was used as a negative control. FISH was also performed to confirm a gain of chromosome 19q shown by CGH. Probe for chromosome region 19p13 was labeled with fluorescein isothiocyanate, and that for 19q13 with Texas Red (clone no. GC180, GSP Laboratory, Inc.) (Supplementary Fig. S1B).

Quantitative RT-qPCR analysis

CDKN2A/B homozygous deletion was investigated by real-time comparative quantitative PCR as well as presence of 9p loss by metaphase CGH. To determine of CDKN2A/B homozygous deletion, six house keeping genes (GAPDH, HMBS, TBP, IPO8, TFRC and YWHAZ) were selected as reference genes. The CNV was calculated by relative changes comparing average of reference genes using the $\Delta\Delta Ct$ method. The RT-qPCR was performed with the

following conditions: 95 ℃ for 120 s, followed by 40 cycles of 95 ℃ for 15 s, 55 ℃ for 15 s, 72 ℃ for 60 s, and melting curve analysis using Fast SYBR® Green Master Mix kit (Applied Biosystems) in ViiA™ 7 Real-Time PCR System (Applied Biosystems). The amplification efficiency of each primer pair (Supplementary Table S2) was evaluated by the standard curve method.

Statistical analysis

One-way ANOVA with post-hoc test was used to compare histological score, Ki-67/MIB-1 index, Nestin-positive cell ratio, and number of CD3, CD8, and PD-1 positive cells among the locations. Chi-square test was used to evaluate extent of resection, recurrence rate, immunohistochemical expression of VEGF-A, VEGFR1/2, PD-L1, and the results of FISH analysis. Progression was defined as radiological evidence of tumor regrowth requiring additional treatment. Progression-free survival (PFS) was calculated from the date of the initial treatment and estimated with the Kaplan–Meier method. The relationship between PFS and each of clinical, histological, and molecular results was analyzed using the log-rank test. We performed univariate and multivariate analyses with Cox regression models to investigate the poor

prognostic factors of PAs. Variables with a *P*-value of < 0.15 were included in a multivariate analysis. Analyses were performed with IBM SPSS statistics (IBM Corp.). A *P* value of < 0.05 was considered statistically significant.

Results

Patient characteristics and tumor location

A total of 38 cases with original institutional diagnosis of PA were included in the study (Table 1). Fourteen out of the 38 tumors occurred in patients younger than 15 years old (defined as pediatric PA) [19]. Tumor location corresponded to the cerebellum in 14 cases, spinal cord in 7, opticohypothalamus in 7, supratentorium in 6, brainstem in 3, and aqueduct in 1 (Fig. 1A). The genetic background of neurofibromatosis type 1 (NF1) was identified in 2 PAs (opticohypothalamus, and aqueduct) and von Hippel-Lindau (VHL) in 1 PA (spinal cord). With a median follow-up of 7 years, 15 cases showed a progressive course; 11

showed a progressive course after surgical resection alone, and 4 after chemo- and/or radio- therapy following surgical resection (Fig. 1B). Three patients were diagnosed as clinically aggressive PA (dorsal pons, spinal cord, and aqueduct). There were three deaths at the time of data fixation (Fig. 1B). The median PFS was 72 months.

There were no significant differences in PFS between adult PAs (≥ 15 years old) and pediatric PAs (< 15 years old) ($P = 0.77$) (Supplementary Fig. S6A). PAs located on the brainstem and spinal cord showed significantly shorter PFS than PAs that occurred at the other sites (brainstem: $P = 0.00076$, spinal cord: $P = 0.021$, both: $P = 0.0015$) (Fig. 1C). Although there was no gross total resection (GTR) in brainstem PAs, the extent of resection was not significantly different among cerebellum, supratentorial, brainstem/spinal cord, and others (opticohypothalamus and aqueduct) ($P = 0.072$) (Table 1). PAs with post-operative treatment and GTR showed significantly shorter and longer PFS than other PAs, respectively (post-operative treatment: $P = 0.0014$, GTR: $P = 0.029$).

Table 1 Clinical characteristics

	N (%)
Age	
≤ 15	14 (37)
> 15	24 (63)
Sex	
Male	22 (58)
Female	16 (42)
Surgery	
GTR	22 (58)
STR	5 (13.2)
PR	8 (21.1)
Biopsy	3 (7.9)
Tumor location/Extent of resection	
Cerebellum	14 (37)/GTR:10, STR:2, PR:2
Supratentorial	6 (16)/GTR: 5, Biopsy:1
Brainstem	3 (8)/STR:1, PR:1, Biopsy:1
Spinal cord	7 (18)/GTR:5, STR:2
Opticohypothalamus	7 (18)/GTR:2, PR:5
Aqueduct	1 (3)/Biopsy:1
Past history	
NF1	2 (5)
VHL	1 (3)
Clinico-pathological classification	
PA	32
CAP	3 (frontal lobe, midbrain, and tectum)
APA	3 (supratentorial, dorsal medulla and midbrain)

APA histological anaplastic pilocytic astrocytomam, *PA* conventional pilocytic astrocytoma, *CAP* clinical aggressive pilocytic astrocytoma, *GTR* gross total removal, *NF1* neurofibromatosis type 1, *PR* partial removal, *STR* subtotal removal, *VHL* von Hippel-Lindau disease

Histopathological analysis

The results of the histopathological and molecular analyses are summarized in Supplementary Table S3 and S6. A neuropathologist (K.O.) reviewed the pathology slides of all 38 tumors and confirmed the diagnosis of PA according to WHO2016. Typical cases with histological high-score and low-score are shown in Fig. 2B. Most cerebellar and opticohypothlamic PAs showed mild nuclear atypia, and either mitosis, endothelial proliferation, or necrosis was not observed in the PAs at those locations. On the other hand, many of the supratentorial, brainstem, and spinal PAs were associated with moderate to marked nuclear atypia, mitosis, and endothelial proliferation. Necrosis was seen only in one supratentorial PA. The histological scores for supratentorial, brainstem, or spinal cord PAs were significantly higher than that of cerebellar PAs (brainstem, $P < 0.01$; supratentorium, $P < 0.01$; spinal cord, $P < 0.05$) (Fig. 2C). Three patients were histologically diagnosed as anaplastic PA (supratentorium, dorsal medulla, and midbrain) with the score 7 for medullary anaplastic PA, 9 for midbrain anaplastic PA, and 9 for occipital one. Unexpectedly, neither the histological high score (≥ 5) nor anaplastic PA was associated with shorter PFS (histological score: $P = 0.41$, APA: $P = 0.68$) (Fig. 2C).

The Ki-67 index for brainstem PAs was significantly higher than that of PAs occurring at the other sites, including the spinal PAs ($P < 0.01$) (Fig. 2D). However, there were no significant differences for PFS between cases with Ki-67 index $\geq 3\%$ and cases with index $< 3\%$ ($P = 0.37$) (Fig. 2D).

IDH1/2, FGFR1, PIK3CA, ATRX, KIAA1549-BRAF fusion, and BRAF-V600E mutation

The *IDH1/2, FGFR1, ATRX, and PIK3CA* mutations were negative in all cases. Twenty of the 38 cases (53%) showed KIAA1549-BRAF fusion; 11 of 14 (79%) cerebellar PAs, 2 of 6 (33%) supratentorial PAs, and 4 of 10 (40%) brainstem/spinal cord PAs were positive for the fusion (Fig. 3A) (Supplementary Table S3 and S6). The positive ratio of cerebellar PAs was significantly higher than that of supratentorial PAs ($P = 0.033$). Two of the 3 anaplastic PAs, and one of the 3 clinically aggressive PAs were positive for KIAA1549-BRAF fusion. BRAF-V600E mutation was observed in 2 tumors—a cerebellar PA and a supratentorial PA. Alterations in the BRAF gene (fusion or mutation) were not associated with prolonged PFS (fusion, $P = 0.23$, mutation, $P = 0.40$, fusion or mutation, $P = 0.29$) (Fig. 3B).

p53 immunohistochemistry

Only 5 cases exhibited positive staining of p53 (1 supratentorial, 2 brainstem, and 2 spinal cord PAs). All 3 anaplastic PAs showed p53-positive staining. PFS of cases with p53-positive staining was significantly shorter than that of cases with p53-negative staining ($P = 0.048$) (Fig. 3C) (Supplementary Table S3 and S6).

Histone H3.3 mutation

Although the histological characteristics were consistent with the diagnosis of PA in all 38 tumors, histone H3.3 mutations were detected by direct sequencing in 2 cases (brainstem PA: H3.3 K27M mutation, spinal cord PA: H3.3 G34R mutation) (Fig. 3D), Supplementary Fig. S3 and S5). The brainstem (midbrain) PA showed moderate cellularity composed of bipolar cells with Rosenthal fibers, and partially showed atypia, mitosis, and endothelial proliferation, which indicated anaplastic PA. On the other hand, the spinal cord PA showed typical PA findings including mild cellularity composed of bipolar cells with Rosenthal fibers, and KIAA1549-BRAF fusion (Supplementary Fig. S5B). As illustrated below, the patient with K27M-mutant midbrain anaplastic PA has been free from tumor progression with radiotherapy and temozolomide/interferon beta for more than two years. The patient with G34R-mutant spinal PA showed tumor recurrence 10 years after the initial surgery followed by radiotherapy, and subsequently suffered from a new brainstem lesion with a pathological diagnosis of sarcoma.

VEGF-A/VEGFRs and nestin expression

Among the 38 cases, 20 cases showed negative VEGF-A staining, and 16 cases were positive. Strong (++) VEGF-A staining was observed in 2 brainstem PAs (clinically aggressive PA and anaplastic PA) (Fig. 4A) (Supplementary Table S3). Eleven cases showed negative VEGFR1 staining, and 27 cases showed + staining (Supplementary Fig. S6B) (Supplementary Table S3 and S6). Five cases showed negative VEGFR2 staining, and 33 cases showed + staining (Supplementary Fig. S6C). All clinically aggressive PAs and anaplastic PAs showed + staining of VEGFR1/2. VEGFR1/2 expression in tumor cells was observed only in the clinically aggressive PAs and anaplastic PAs. PFS of cases with positive VEGF-A expression was significantly shorter than that of cases with negative expression ($P = 0.045$) (Fig. 4A). VEGFR1 or VEGFR2 expression was not related to PFS (VEGFR1, $P = 0.35$, VEGFR2, $P = 0.41$) (Supplementary Fig. S6B, C). Although there was no significant difference in VEGF-A and VEGFR1/2 expression among the 5 locations (VEGF-A, $P = 0.12$, VEGFR1, $P = 0.22$, VEGFR2, $P = 0.24$) (Fig. 4A, Supplementary Fig. S6B, C), all 3 brainstem PAs were positive for all of the VEGF-A and VEGFR1/2.

The Nestin-positive cell ratio was below 10% in most cases. However, the ratio of brainstem PAs was significantly higher than that of the other PAs ($P < 0.01$)
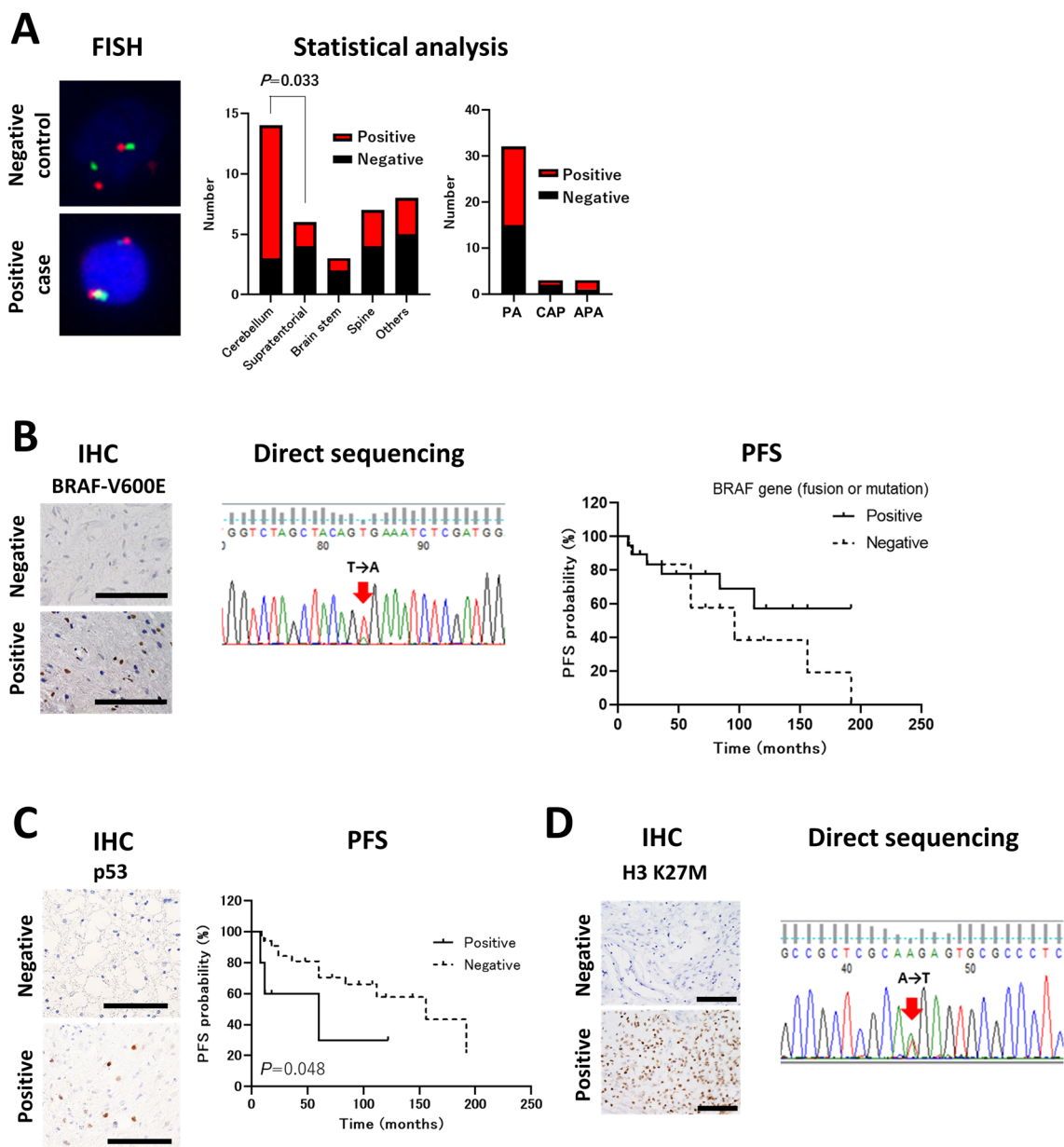
Fig. 3 Molecular analysis. **A** Left panel: FISH analysis of KIAA1549-BRAF fusion. Right panel: The number of positive and negative PA cases with KIAA1549-BRAF fusion per location and subsets (PA, CAP and APA). **B** Left panel: Immunohistochemical expression of BRAF-V600E. Middle panel: Determination of the BRAF V600E mutation in tumor specimens through direct sequencing. Right panel: Kaplan–Meier curve of PFS according to the status of BRAF fusion or mutation. **C** Left panel: Immunohistochemical expression of p53. Right panel: Kaplan–Meier curve of PFS according to p53 status. Scale bar, 100 μm. **D** Left panel: Immunohistochemical expression of H3 K27M. Right panel: Determination of the H3 K27M mutation in tumor specimens through direct sequencing. Scale bar, 100 μm. *PA* conventional pilocytic astrocytoma, *CAP* clinically aggressive PA, *APA* histologically anaplastic PA

(Fig. 4B). All clinically aggressive PAs and one anaplastic PA in the dorsal medulla showed quite high Nestin-positive cell ratio ($\geq 15\%$). PFS of cases with high Nestin-positive cell ratio ($\geq 10\%$) was significantly shorter than that of cases with low ratio ($P = 0.0035$) (Fig. 4B).

CD3, CD8, PD-1 and PD-L1 expression

As for the tumor immune-microenvironment, the density of CD3$^+$ and CD8$^+$ T cells was low in most PAs as compared with higher grade gliomas (CD3, 20 cases were $\leq 15/5$ HPF;

Fig. 4 Angiogenesis, stemness, and tumor immune-micro-environment. **A** Upper left panel: Immunohistochemical expression of VEGF-A. Lower left panel: The number of positive and negative PA cases with VEGF-A expression per location and subsets (PA, CAP and APA). Upper right panel: Kaplan–Meier curve of PFS according to VEGF-A status. Scale bar, 50 μm. **B** Upper left panel: Immunohistochemical expression of Nestin. Lower left panel: Nestin-positive cell ratio per location and subsets (PA, CAP, and APA). Upper right panel: Kaplan–Meier curve of PFS according to the status of Nestin. Scale bar, 50 μm. **C** Upper left panel: Immunohistochemical expression of PD-L1. Lower left panel: The number of low and high score PA cases with PD-L1 expression per location and subset (PA, CAP, and APA). Upper right panel: Kaplan–Meier curve of PFS according to PD-L1 status. Scale bar, 50 μm. *PA* conventional pilocytic astrocytoma, *CAP* clinically aggressive PA, *APA* histologically anaplastic PA
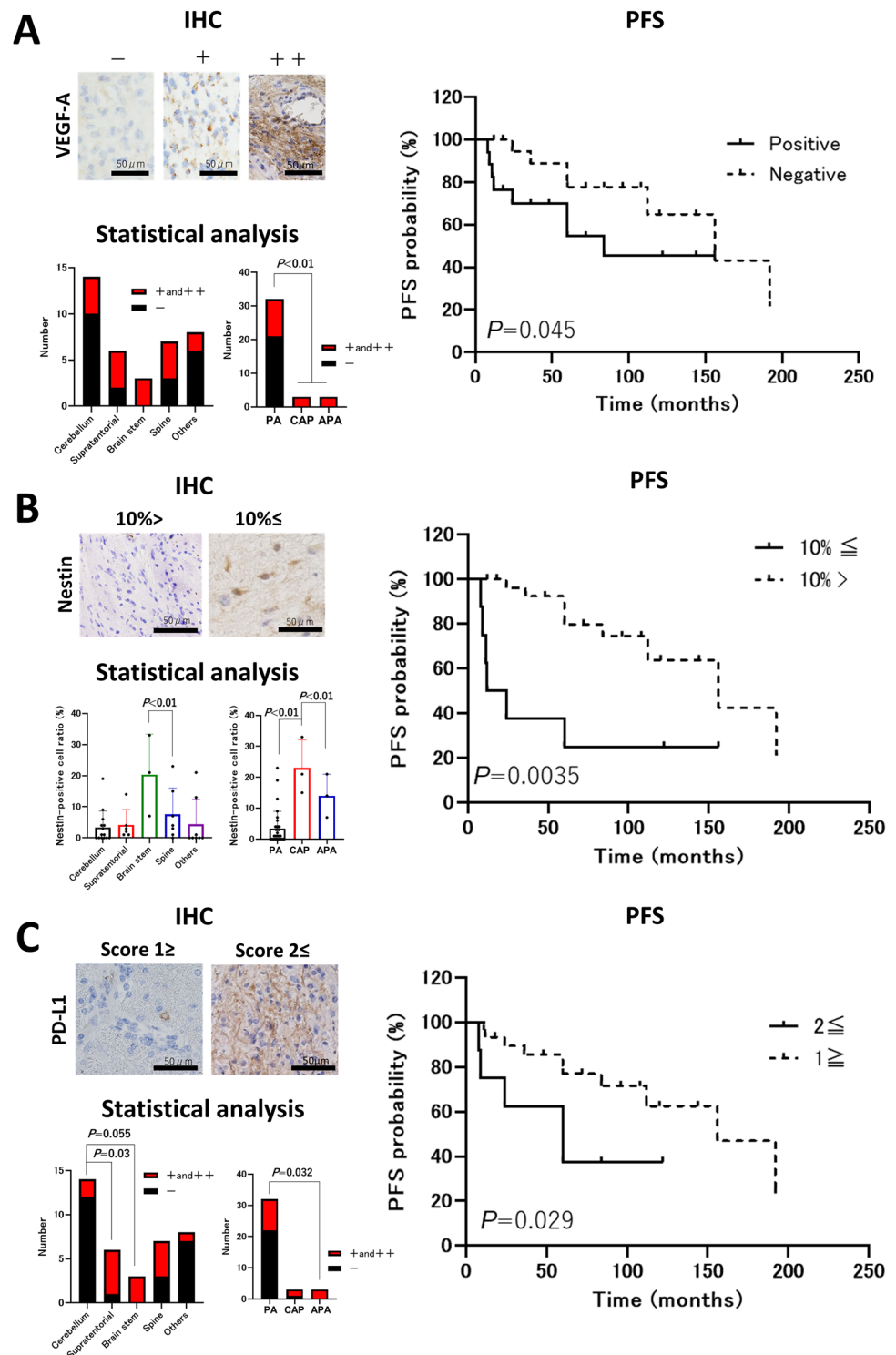
CD8, 30 cases were $\leq 15/5$ HPF) [12]. Tumor location was not associated with the number of CD3$^+$ or CD8$^+$ T cells (Supplementary Fig. S6D, E) (Supplementary Table S3). The number of CD3$^+$ or CD8$^+$ T cells was not associated with PFS (Supplementary Fig. S6D, E). The number of PD-1$^+$ cells in the brainstem or supratentorial PAs was significantly higher than that of other PAs ($P < 0.05$ for each), however, PD-1 expression was not associated with PFS (Supplementary Fig. S6F).

A total of 23 of the 38 tumors were PD-L1-negative. The supratentorial and brainstem PAs were more frequently PD-L1-positive than the cerebellar PAs (supratentorium,

$P = 0.03$, brainstem, $P = 0.055$) (Fig. 4C), and all 3 anaplastic PAs were PD-L1-positive. PFS of cases with high PD-L1 score (≥ 2) was significantly shorter than that of cases with scores of 0 and 1 ($P = 0.029$) (Fig. 4C).

Chromosomal number aberrations by metaphase CGH

Nine of the 38 cases showed chromosomal number aberrations (CNAs) (7 adult PAs, and 2 pediatric PAs). Gain of chromosome 7q was detected in one brainstem anaplastic PA, one aqueduct clinically aggressive PA (Fig. 5A), and 3 of the 7 spinal PAs. Six of the 7 spinal PAs exhibited gain of chromosome 19 which was confirmed by FISH analysis in 5 cases where extra samples were available (Fig. 5B). PFS of PAs with copy number gain of chromosome 7q and/or 19 was significantly shorter than that of the other PAs (7q gain, $P = 0.0027$; 19 gain, $P = 0.026$; gain of both, $P = 0.00030$) (Fig. 5C). Loss of chromosome 9p21, the gene locus for the CDKN2A gene was detected in a case of histologically anaplastic PA (Supplementary Fig S2). CDKN2A/B homozygous deletion was also verified multiplex ligation-dependent probe amplification analysis.

Univariate and multivariate analyses for prognostic factors

The data from all cases are summarized in Supplementary Table S6. To determine the poor prognostic factors in PAs, we performed univariate analysis with Cox regression models for the factors that were shown to be associated with patient PFS by Kaplan Meier analysis and log-rank test: the brainstem/spinal cord location, extent of resection and post-operative treatment among the clinical factors, and p53 expression, VEGF-A expression, Nestin-positive cell ratio ($\geq 10\%$ vs. $< 10\%$), PD-L1 score (1 and 2 vs. 0), and CNAs (a gain of copy number with chromosome region 7q and/or 19 vs. others) among molecular factors. As a result, brainstem/spinal location, extent of removal, postoperative treatment, nestin-positive cell ratio, and gain of either 7q or 19 were significantly associated with shorter PFS (Table 3). Subsequently, to exclude the impact of possible confounding factors due to clinical heterogeneity, we performed multivariate analysis with the above molecular factors and extent of resection (GTR vs others), post-operative treatment (wait and see vs either chemotherapy or radiotherapy), or brainstem/spinal location; the Nestin-positive cell ratio, CNAs, and extent of removal were independent predictors of poor prognosis (Table 3).

The characteristics of all clinically aggressive PAs in the present studies are summarized in Table 2. All 3 clinically aggressive PAs showed at least 2 molecular prognostic factors confirmed by multivariate analyses, and, indeed, high

expression of Nestin positive cell ratio was shared in all of the 3 tumors. For example, a clinically aggressive PA with a cyst on the dorsal pons demonstrated $++$ staining of VEGF-A, as well as 33% of Nestin-positive cells (Supplementary Fig. S4A, B).

Moreover, it should be noted that 2 of the 3 clinically aggressive PAs occurred in the patients with hereditary genetic disease (NF1 and VHL).

Illustrative cases

Two cases of anaplastic PAs that showed contrasting clinical course and a case of spinal PA with H3.3 G34 mutation was detailed in the Supplementary files (Supplementary Fig. S2, 3, and 5).

Discussion

In the present study, 38 PAs were investigated for the relevance to tumor recurrence by comprehensive analyses of clinical, histological and molecular factors which were previously known to be possibly associated with tumorigenesis or progression of gliomas. The study demonstrated that the extent of resection, post-operative treatment, brainstem/spinal location, TP53 mutation, VEGF pathway, Nestin expression, PD-/PD-L1 immune checkpoint, and chromosomal gain of 7q or 19, but neither histological features nor Ki-67 index, might be associated with aggressiveness of the tumor, with the majority of which being the first to report to our knowledge. Importantly, the Nestin-positive cell ratio, CNAs, and extent of removal were suggested to be independent predictors of poor prognosis by multivariate analyses. Moreover, the study also showed that PAs in the brainstem or spinal cord might be associated with distinct molecular characteristics including those listed above, leading to the aggressive clinical course shown by the univariate analysis.

The significance of anaplastic features as well as the Ki-67 index was controversial in PAs. Rodriguez et al. reported that, in their analysis of 34 cases of anaplastic PAs, anaplastic PA was associated with a worse prognosis as compared with PAs [2]. However, other reports have demonstrated that the clinical course of anaplastic PA was perceived as more favorable [20, 21]. Similarly, Ki-67 index was typically below 1% in PAs, and several investigators reported that PAs with high Ki-67 index were associated with a shorter PFS [22, 23]. However, some cases showed poor prognosis despite the low Ki-67 index [24]. In this study, neither the histological score nor Ki-67 was shown to be associated with the patients' PFS. Indeed, 2 of the 3 patients with anaplastic PAs did not show a progressive course, and histological diagnosis of anaplastic PA was not associated with shorter PFS. Thus, although PAs with
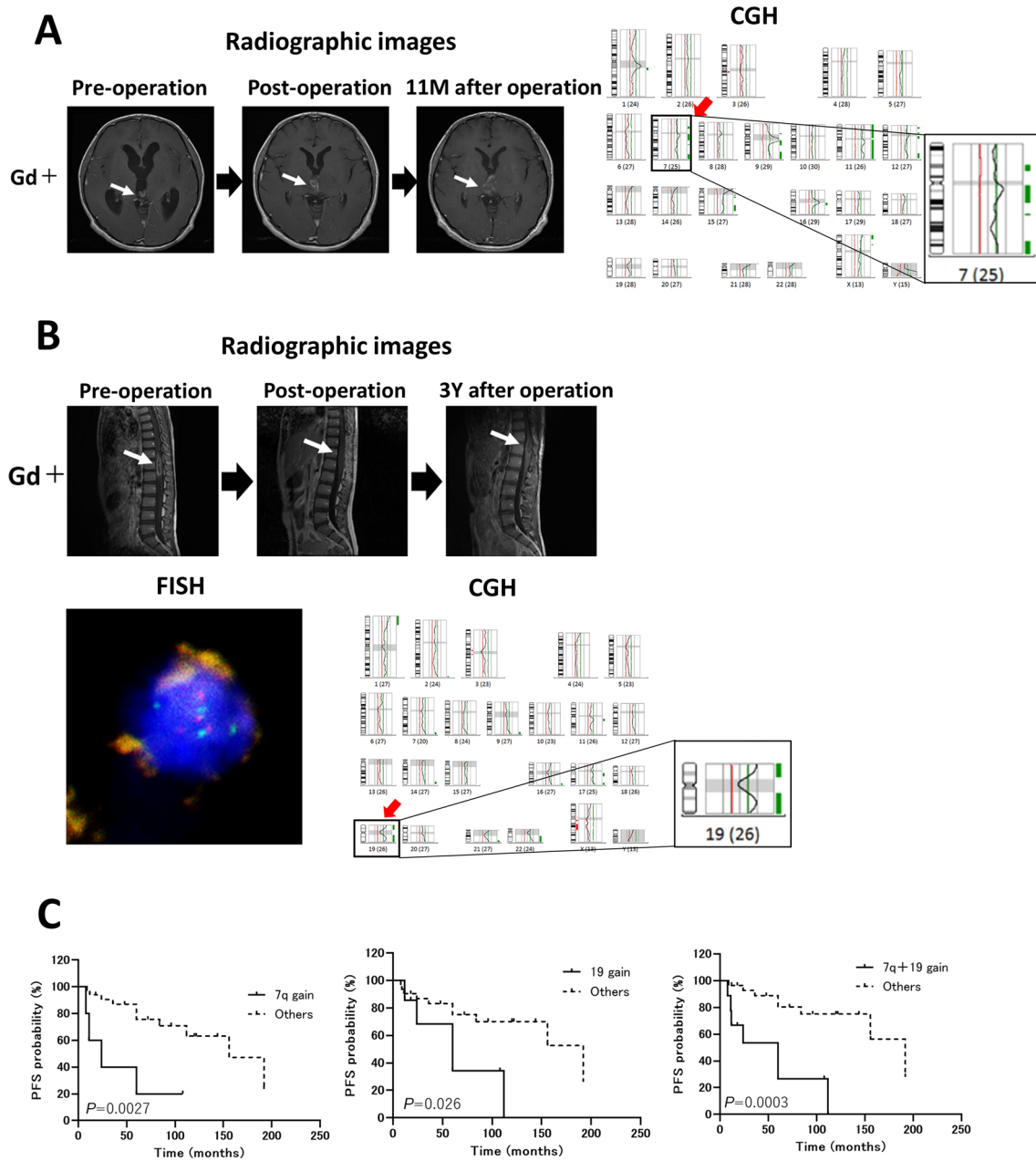
Fig. 5 CGH analysis. **A** Left panel: The PA located on the aqueduct has rapidly enlarged over the 11 months after the operation (white arrow). Right panel: A gain of copy number with chromosome region 7q is detected (red arrow). **B** Upper panel: Spinal PA shows recurrence 3 years after surgery (white arrow). Lower left panel: Two copy number gain of chromosome is also confirmed with FISH analysis. Lower right panel: A gain of copy number with chromosome region 19 is detected (red arrow). **C** Kaplan–Meier curve of PFS according to the status of 7q and/or 19 gain

histological characteristics of malignancy should be carefully treated and observed, the biological behavior of PAs appear to be difficult to be predicted only from histological findings.

Although VEGF-A/VEGFRs expression was typically low in PAs as compared with high-grade gliomas [5, 25], in the present study, the expression of VEGF was noted in approximately one third of PAs, that of VEGFR1 in about two thirds, and VEGFR2 in the majority of cases. Importantly, positive VEGF expression was significantly associated with shorter PFS in univariate analysis. All clinically aggressive PAs were positive for VEGF, VEGFR1, and VEGFR2 (Supplementary Table S5). These data suggest that angiogenesis involving the VEGF pathway might be relevant to the aggressive biological behavior of PAs.

Table 2 Summary of CAPs

	Age/Sex	Location	PH	HS	P53	Ki-67 Index (%)	BRAF mutation/fusion	CGH	Other findings	PFS (post-operative treatment)
CAP1	14/F	Dorsal pons	–	3	No	3	No/no	No	PD-L1 score≥2 Nestin ratio>15% VEGF-A: ++	9 m (chemotherapy)
CAP2	19/M	Aqueduct	NF1	3	No	1	No/no	7q gain	Nestin ratio>15%	11 m (Wait-and-scan management)
CAP3	40/M	spinal cord	VHL	4	Yes	5	No/yes	19 gain	Nestin ratio>15% TP 53 mutation: +	12 m (radiotherapy)

Two out of 3 CAPs were associated with genetic disease (NF1 and VHL), and had CNAs. Although all CAPs showed low histological score and Ki-67 index, the Nestin-positive cell ratio was much higher than that of typical PAs. One CAP with a cyst on the dorsal pons demonstrated + + staining of VEGF-A, as well as 33% of Nestin-positive cells. PFS of CAPs were significantly shorter than that of other PAs ($P < 0.001$)

CAP clinical aggressive pilocytic astrocytoma, *CGH* Comparative genomic hybridization, *HS* histological score, *NF1* neurofibromatosis type 1, *PD-L1* programmed death-ligand 1, *PFS* progression-free survival, *PH* past history, *VEGF* vascular endothelial growth factor, *VHL* von Hippel-Lindau

Table 3 Cox proportional hazards model for progression-free survival

Variables		Univariate analysis			Multivariate analysis with extent of removal			Multivariate analysis with postoperative treatment			Multivariate analysis with brainstem/spinal location		
		HR	95% CI	P value	HR	95% CI	P value	HR	95% CI	P value	HR	95% CI	P value
5 Molecules	P53	3.09	0.84–11.34	0.13									
	VEGF-A	2.23	0.77–6.47	0.14									
	Nestin	4.26	1.46–12.43	0.013	4.36	1.36–14.04	0.018	4.91	1.54–15.65	0.0098	4.79	1.51–15.23	0.0079
	PD-L1	2.59	0.85–7.86	0.094									
	CGH	5.81	1.93–17.44	0.0025	6.52	1.97–21.60	0.0027	4.19	1.17–14.99	0.028	3.79	0.29–49.86	0.31
Extent of removal		0.32	0.11–0.96	0.037	0.28	0.087–0.92	0.031						
Postoperative treatment		4.59	1.64–12.88	0.0049				2.48	0.78–7.82	0.12			
Brainstem/spinal location		4.87	1.62–14.67	0.0061							1.76	0.13–2293	0.67

CGH metaphase comparative genomic hybridization, *CI* confidence interval, *HR* hazard ratio, *PD-L1* programmed cell death-ligand 1, *VEGF-A* vascular endothelial growth factor-A

The level of Nestin expression correlates with the grade of malignancy in malignant glioma [4]. Although Nestin expression is generally low in PAs [26], moderate Nestin expression is occasionally identified in PAs [27]. Importantly, high Nestin-positive cell ratio ($\geq 10\%$) was an independent predictor of early recurrence in this study (Table 3). Indeed, all clinically aggressive PAs were associated with high Nestin positive cell ratio (Table 2). Therefore, Nestin expression is likely to be an indicator of aggressive clinical course in PAs.

There are few reports regarding the tumor immune-microenvironment in PAs [28–30]. There was no association between PD-L1 expression and patients' prognosis in a previous study with 10 cases of PAs [30]. Conversely, although PD-L1 expression was not detected in most PAs in this study, 8 PAs with high PD-L1 expression were associated with shorter PFS. Indeed, the aggressive anaplastic PA located on the dorsal medulla showed an extremely high expression of the cancer immunity-associated molecules/cells including PD-L1 (Supplementary Fig. S2). These findings suggest that the immune-microenvironment including PD-1/PD-L1 signaling might be associated with aggressiveness of PAs.

Almost all PAs show abnormality in the MAPK pathway mostly caused by KIAA1549-BRAF fusion and point mutation of BRAF-V600E [1]. The prognostic impact of KIAA1549-BRAF fusion is controversial [31–33]. In the present study, although there was no significant difference, there might be a trend towards favorable PFS in the cases with BRAF alterations; lack of statistical significance might be attributable to the small number of cases included in the study.

CNAs are rarely found in PAs; however, gains of chromosomes 5, 6, and 7 and losses of chromosomes 16, 17, 19, and 22 have been reported previously [34, 35]. Whole chromosome 7 gain was more frequent in patients aged 16 years and older and was significantly associated with tumor recurrence [35]. In the present study, there was no PA with gain of 7 (whole), however, gain of 7q was significantly associated with a shorter PFS. Moreover, a gain of chromosome 19 was detected in 6 out of the 7 spinal PAs and was also associated with shorter PFS. The gain of 19 has rarely been reported in PAs in the literature [36–38] and was exclusively detected in spinal PAs in the present study. Because the rate of GTR did not differ between cerebellar and spinal PAs, gain of chromosome 19 could partly account for the relative poor prognosis of patients with spinal PAs as compared with cerebellar PAs. There are some genes and genetic locus implicated in cancer development on chromosome 19 mentioned in the literature, such as AKT2, cyclin E and MLL2 at 19q13 [39–42].

TP53 mutation is rare in PAs [43], but it is a common observation in anaplastic PAs (Supplementary Table S3)

[2, 21, 44–58]. Indeed, in this study, 5 cases were positive for p53 staining; 3 anaplastic PAs, 1 clinically aggressive PA, and 1 PA with recurrence, and p53 staining were significantly associated with shorter PFS. Therefore, TP53 mutation is likely relevant to the aggressiveness as well as histological anaplasia of PAs [59]. However, TP53 mutation was not significant at the multivariate level, which may be associated with the small number of the patients.

Reports of PAs with H3 mutation raise the issue of differential diagnosis from diffuse midline glioma, H3K27M-mutant, which is associated with poor prognosis regardless of the histological appearance and is thus designated as WHO grade IV [60, 61]. In 4 previous studies, H3K27M mutation was not detected in a total of 154 PAs [62–65]; however, recently, PAs with H3K27M mutation have been reported (Supplementary Table S4) [66–72]. According to the recommendation by the cIMPACT-NOW, circumscribed glial tumors such as PA and ganglioglioma with H3 mutation do not meet the criteria of diffuse midline glioma [73]. However, a meta-analysis showed that H3K27M mutation remained the prognostic factor for poor survival in circumscribed gliomas [74]. Furthermore, among the 11 PAs with H3K27M mutation found in the literature (Supplementary Table S4), 6 were associated with tumor recurrence or poor prognosis. In the present study, a midbrain PA with H3K27M mutation survives more than 2.3 years after initial resection, suggesting a better clinical course as compared with diffuse glioma with the same mutation (Supplementary Fig. S3). However, the tumor was slowly progressive on serial MRIs, and the patient is being observed closely. In the present study, a spinal PA showed a H3G34R mutation. The patient had tumor recurrence 10 years after initial resection, and eventually died 2 years after recurrence. H3G34 mutant glioblastomas typically occur in the cerebral hemispheres in adolescents and young adults [63, 64]. To our knowledge, this study is the first to report G34R mutation in PAs and in spinal tumors. Further analysis is needed to discuss the prognosis of PAs with H3G34 mutation.

The five-year survival rate of spinal cord PAs was 81%-85.4%, according to the literature, which was slightly lower than that for cerebellar PAs [75]. In this study, in line with previous studies, PAs located on the brainstem and spinal cord were associated with shorter PFS than the other PAs. There were several differences in molecular findings between brainstem or spinal PAs and those of the other sites, especially in terms of cerebellar PAs (Supplementary Table S3); the Nestin-positive cell ratio of brainstem PAs was significantly higher than those of PAs arising in the other sites, the number of PD-1 + cells in brainstem or supratentorial PAs was significantly higher than that of other PAs, brainstem PAs were more frequently positive for PD-L1 than cerebellar PAs. Moreover, CNAs were almost exclusively found in brainstem/spinal PAs (Supplementary

Table S3). Therefore, brainstem/spinal PAs appear to have distinct molecular characteristics as compared with those arising at the other sites, which likely accounts for relatively aggressive clinical course.

Importantly, Reinhardt et al. [76] reported that significant proportion of histologically anaplastic PAs constitutes a separate DNA methylation cluster, leading to the new tumor type designated as high-grade astrocytoma with piloid features (HGAP, WHO 2021 [8]). Currently, DNA methylation profiling is the only method for definitive diagnosis of HGAP, and the most common molecular alterations in those tumors were deletions of CDKN2A/B, MAPK pathway gene alterations, and mutations of ATRX or loss of ATRX mutations. We regret that DNA-methylation profiling has not been available in the current study. It is notable that deletions of CDKN2A/B were observed in a case of histologically anaplastic PA with KIAA1549-BRAF fusion, suggesting that the case was likely to be HGAP (Supplementary Fig S2).

Limitation of the study

The major limitation of the present study includes the retrospective study design, small sample size, and heterogeneity in post-operative treatment. In particular, studies using a larger number of patients with rare categories (anaplastic PAs and clinically aggressive PAs) are warranted in order to confirm the findings of this study. Nonetheless, the study with multistep analyses clearly showed relevance of some molecular factors to the recurrence of PAs and those factors are likely associated with the distinct biological behavior of the brainstem and spinal PAs.

Conclusions

The present study demonstrated that some molecular factors, rather than histological parameters, may be associated with aggressiveness of PAs, including TP53 mutation, upregulation of VEGF pathway, upregulation of PD-1/PD-L1 immune checkpoint, Nestin expression and gains of 7q and 19. On the other hand, among the clinical factors, the extent of resection, postoperative treatment, brainstem/spinal location were suggested to be associated with early tumor recurrence. PAs with those characteristics may be succumb to early tumor recurrence, and, patients with those tumors should be more carefully managed than the others.

Declarations

References

1. Collins VP, Jones DT, Giannini C (2015) Pilocytic astrocytoma: pathology, molecular mechanisms and markers. Acta Neuropathol 129:775–788
2. Rodriguez FJ, Scheithauer BW, Burger PC et al (2010) Anaplasia in pilocytic astrocytoma predicts aggressive behavior. Am J Surg Pathol 34:147–160
3. Rodriguez EF, Scheithauer BW, Giannini C et al (2011) PI3K/AKT pathway alterations are associated with clinically aggressive and histologically anaplastic subsets of pilocytic astrocytoma. Acta Neuropathol 121:407–420
4. Arai H, Ikota H, Sugawara K et al (2012) Nestin expression in brain tumors: its utility for pathological diagnosis and correlation with the prognosis of high-grade gliomas. Brain Tumor Pathol 29:160–167
5. Schmidt NO, Westphal M, Hagel C et al (1999) Levels of vascular endothelial growth factor, hepatocyte growth factor/scatter factor and basic fibroblast growth factor in human gliomas and their relation to angiogenesis. Int J Cancer 84:10–18
6. Kamamoto D, Ohara K, Kitamura Y et al (2018) Association between programmed cell death ligand-1 expression and extracranial metastasis in intracranial solitary fibrous tumor/hemangiopericytoma. J Neurooncol 139:251–259
7. Louis DN, Perry A, Reifenberger G et al (2016) The 2016 world health organization classification of tumors of the central nervous system: a summary. Acta Neuropathol 131:803–820
8. WHO Classification of Tumours. Louis DN, Perry A, Wesseling P, Brat DJ, et al (2021) Central nervous system tumours. Lyon (France): International Agency for Research on Cancer. (WHO

classification of tumours series, 5th ed.; vol. 6). Available from: https://tumourclassification.iarc.who.int/chapters/45. Accessed 3 May 2022.

9. Tamura R, Miwa T, Ohira T, Yoshida K (2017) Diagnosis and treatment for pure aqueductal tumor. J Clin Neurosci 44:260–263

10. Roth J, Chaichana KL, Jallo G et al (2015) True aqueductal tumors: a unique entity. Acta Neurochir (Wien) 157:169–177

11. Tamura R, Tanaka T, Miyake K et al (2016) Histopathological investigation of glioblastomas resected under bevacizumab treatment. Oncotarget 7:52423–52435

12. Tamura R, Tanaka T, Ohara K et al (2019) Persistent restoration to the immunosupportive tumor microenvironment in glioblastoma by bevacizumab. Cancer Sci 110:499–508

13. Takami H, Yoshida A, Fukushima S et al (2015) Revisiting TP53 mutations and immunohistochemistry—a comparative study in 157 diffuse gliomas. Brain Pathol 25:256–265

14. Hirose Y, Aldape K, Takahashi M et al (2001) Tissue microdissection and degenerate oligonucleotide primed-polymerase chain reaction (DOP PCR) is an effective method to analyze genetic aberrations in invasive tumors. J Mol Diagn 3:62–67

15. Sasaki H, Zlatescu MC, Betensky RA et al (2001) PTEN is a target of chromosome 10q loss in anaplastic oligodendrogliomas and PTEN alterations are associated with poor prognosis. Am J Pathol 159:359–367

16. Schindler G, Capper D, Meyer J et al (2011) Analysis of BRAF V600E mutation in 1320 nervous system tumors reveals high mutation frequencies in pleomorphic xanthoastrocytoma, ganglioglioma and extra-cerebellar pilocytic astrocytoma. Acta Neuropathol 121:397–405

17. Yan H, Parsons DW, Jin G et al (2009) IDH1 and IDH2 mutations in gliomas. N Engl J Med 360:765–773

18. Kitamura Y, Komori T, Shibuya M et al (2018) Comprehensive genetic characterization of rosette-forming glioneuronal tumors: independent component analysis by tissue microdissection. Brain Pathol 28:87–93

19. Khan MA, Godil SS, Tabani H et al (2012) Clinical review of pediatric pilocytic astrocytomas treated at a tertiary care hospital in Pakistan. Surg Neurol Int 3:90

20. Sugita Y, Nakashima S, Ohshima K et al (2013) Anaplastic astrocytomas with abundant Rosenthal fibers in elderly patients: a diagnostic pitfall of high-grade gliomas. Neuropathology 33:533–540

21. Saito K, Toda M, Yoshida K (2015) Pilocytic astrocytoma with anaplastic features presenting good long-term clinical course after surgery alone: a case report. Childs Nerv Syst 31:167–171

22. Bowers DC, Gargan L, Kapur P, Reisch JS (2003) Study of the MIB-1 labeling index as a predictor of tumor progression in pilocytic astrocytomas in children and adolescents. J Clin Oncol 21:2968–2973

23. Casadei GP, Arrigoni GL, D'Angelo V, Bizzozero L (1990) Late malignant recurrence of childhood cerebellar astrocytoma. Clin Neuropathol 9:295–298

24. Ito S, Hoshino T, Shibuya M et al (1992) Proliferative characteristics of juvenile pilocytic astrocytomas determined by bromodeoxyuridine labeling. Neurosurgery 31:413–418

25. Mustafa D, Swagemakers S, French P et al (2013) Structural and expression differences between the vasculature of pilocytic astrocytomas and glioblastomas. J Neuropathol Exp Neurol 72:1171–1181

26. Almqvist PM, Mah R, Lendahl U et al (2002) Immunohistochemical detection of nestin in pediatric brain tumors. J Histochem Cytochem 50:147–158

27. Kitai R, Horita R, Sato K et al (2010) Nestin expression in astrocytic tumors delineates tumor infiltration. Brain Tumor Pathol 27:17–21

28. Zeng J, Zhang XK, Chen HD et al (2016) Expression of programmed cell death-ligand 1 and its correlation with clinical outcomes in gliomas. Expression of programmed cell death-ligand 1 and its correlation with clinical outcomes in gliomas. Oncotarget 7:8944–8955

29. Yang I, Han SJ, Sughrue ME et al (2011) Immune cell infiltrate differences in pilocytic astrocytoma and glioblastoma: evidence of distinct immunological microenvironments that reflect tumor biology. J Neurosurg 115:505–511

30. Wei B, Wang L, Zhao X et al (2014) The upregulation of programmed death 1 on peripheral blood T cells of glioma is correlated with disease progression. Tumour Biol 35:2923–2929

31. Hawkins C, Walker E, Mohamed N et al (2011) BRAF-KIAA1549 fusion predicts better clinical outcome in pediatric low-grade astrocytoma. Clin Cancer Res 17:4790–4798

32. Horbinski C, Hamilton RL, Nikiforov Y, Pollack IF (2010) Association of molecular alterations, including BRAF, with biology and outcome in pilocytic astrocytomas. Acta Neuropathol 119:641–649

33. Tihan T, Ersen A, Qaddoumi I et al (2012) Pathologic characteristics of pediatric intracranial pilocytic astrocytomas and their impact on outcome in 3 countries: a multi-institutional study. Am J Surg Pathol 36:43–55

34. Forshew T, Tatevossian RG, Lawson AR et al (2009) Activation of the ERK/MAPK pathway: a signature genetic defect in posterior fossa pilocytic astrocytomas. J Pathol 218:172–181

35. Sanoudou D, Tingby O, Ferguson-Smith MA et al (2010) Analysis of pilocytic astrocytoma by comparative genomic hybridization. Br J Cancer 82:1218–1222

36. Roth JJ, Fierst TM, Waanders AJ et al (2016) Whole chromosome 7 gain predicts higher risk of recurrence in pediatric pilocytic astrocytomas independently from KIAA1549-BRAF fusion status. J Neuropathol Exp Neurol 75:306–315

37. Roberts P, Chumas PD, Picton S et al (2001) Review of the cytogenetics of 58 pediatric brain tumors. Cancer Genet Cytogenet 131:1–12

38. Sanoudou D, Tingby O, Ferguson-Smith MA et al (2000) Analysis of pilocytic astrocytoma by comparative genomic hybridization. Br J Cancer 82:1218–1222

39. Alvarez S, MacGrogan D, Calasanz MJ et al (2001) Frequent gain of chromosome 19 in megakaryoblastic leukemias detected by comparative genomic hybridization. Genes Chromosomes Cancer 32:285–293

40. Kuuselo R, Simon R, Karhu R et al (2010) 19q13 amplification is associated with high grade and stage in pancreatic cancer. Genes Chromosomes Cancer 49:569–575

41. Ogawa K, Osanai M, Obata M et al (1999) Gain of chromosomes 15 and 19 is frequent in both mouse hepatocellular carcinoma cell lines and primary tumors, but loss of chromosomes 4 and 12 is detected only in the cell lines. Carcinogenesis 20:2083–2088

42. Wang X, Zhang Y, Nilsson CL et al (2015) Erratum to: association of chromosome 19 to lung cancer genotypes and phenotypes. Cancer Metastasis Rev 34:227

43. Matsumoto T, Fujii T, Yabe M et al (1998) MIB-1 and p53 immunocytochemistry for differentiating pilocytic astrocytomas and astrocytomas from anaplastic astrocytomas and glioblastomas in children and young adults. Histopathology 33:446–452

44. Azad A, Deb S, Cher L (2009) Primary anaplastic pilocytic astrocytoma. J Clin Neurosci 16:1704–1706

45. Ballester LY, Penas-Prado M, Leeds NE et al (2018) FGFR1 tyrosine kinase domain duplication in pilocytic astrocytoma with anaplasia. Cold Spring Harb Mol Case Stud 4:a002378

46. Fiechter M, Hewer E, Knecht U et al (2016) Adult anaplastic pilocytic astrocytoma – a diagnostic challenge? A case series and literature review. Clin Neurol Neurosurg 147:98–104

47. Hayashi S, Akao N, Nakazato Y (2017) Pilocytic astrocytoma with anaplasia arising from the optic chiasm in a very elderly patient. Neurology 89:1840

48. Hsieh MS, Ho JT, Lin LW et al (2012) Cerebellar anaplastic pilocytic astrocytoma in a patient of neurofibromatosis type-1: case report and review of the literature. Clin Neurol Neurosurg 114:1027–1029

49. Ishii N, Sawamura Y, Tada M et al (1998) Absence of p53 gene mutations in a tumor panel representative of pilocytic astrocytoma diversity using a p53 functional assay. Int J Cancer 76:797–800

50. Kraus JA, Wenghoefer M, Schmidt MC et al (2000) Long-term survival of glioblastoma multiforme: importance of histopathological reevaluation. J Neurol 247:455–460

51. Lach B, Al Shail E, Patay Z (2003) Spontaneous anaplasia in pilocytic astrocytoma of cerebellum. Br J Neurosurg 17:250–252

52. Shibahara I, Kawaguchi T, Kanamori M et al (2011) Pilocytic astrocytoma with histological malignant features without previous radiation therapy–case report. Neurol Med Chir (Tokyo) 51:144–147

53. Shinoura N, Takahashi M, Yamada R (2006) Delineation of brain tumor margins using intraoperative sononavigation: implications for tumor resection. J Clin Ultrasound 34:177–183

54. Srinivas BH, Rajesh A, Shukla D (2016) Spontaneous anaplastic transformation in cerebellar pilocytic astrocytoma: a case report and review of literature. IOSR J Dental Med Sci 15:53–56

55. Stuer C, Vilz B, Majores M et al (2007) Frequent recurrence and progression in pilocytic astrocytoma in adults. Cancer 110:2799–2808

56. Trabelsi S, Mama N, Ladib M et al (2015) Adult recurrent pilocytic astrocytoma: clinical, histopathological and molecular study. Neurochirurgie 61:392–397

57. Tsuda K, Ishikawa E, Saito A et al (2011) Primary cerebellar pilocytic astrocytoma with anaplastic features in a patient with neurofibromatosis type 1 - case report -. Neurol Med Chir (Tokyo) 51:315–318

58. Yong EX, McKelvie P, Murphy M, Wang YY (2014) Anaplastic pilocytic astrocytoma. J Clin Neurosci 21:1993–1996

59. Hayes VM, Dirven CM, Dam A et al (1999) High frequency of TP53 mutations in juvenile pilocytic astrocytomas indicates role of TP53 in the development of these tumors. Brain Pathol 9:463–467

60. Solomon DA, Wood MD, Tihan T et al (2016) Diffuse midline gliomas with histone H3–K27M mutation: a series of 47 cases assessing the spectrum of morphologic variation and associated genetic alterations. Brain Pathol 26:569–580

61. Sturm D, Witt H, Hovestadt V et al (2012) Hotspot mutations in H3F3A and IDH1 define distinct epigenetic and biological subgroups of glioblastoma. Cancer Cell 22:425–437

62. Gielen GH, Gessi M, Hammes J (2013) H3F3A K27M mutation in pediatric CNS tumors: a marker for diffuse high-grade astrocytomas. Am J Clin Pathol 139:345–349

63. Schwartzentruber J, Korshunov A, Liu XY et al (2012) Driver mutations in histone H3.3 and chromatin remodelling genes in paediatric glioblastoma. Nature 482:226–231

64. Wu G, Broniscer A, McEachron TA et al (2012) Somatic histone H3 alterations in pediatric diffuse intrinsic pontine gliomas and non-brainstem glioblastomas. Nat Genet 44:251–253

65. Zhang J, Wu G, Miller CP et al (2013) Whole-genome sequencing identifies genetic alterations in pediatric lowgrade gliomas. Nat Genet 45:602–612

66. Hochart A, Escande F, Rocourt N et al (2015) Long survival in a child with a mutated K27M–H3.3 pilocytic astrocytoma. Ann Clin Transl Neurol 2:439–443

67. Morita S, Nitta M, Muragaki Y et al (2018) Brainstem pilocytic astrocytoma with H3 K27M mutation: case report. J Neurosurg 129:593–597

68. Orillac C, Thomas C, Dastagirzada Y et al (2016) Pilocytic astrocytoma and glioneuronal tumor with histone H3 K27M mutation. Acta Neuropathol Commun 4:84

69. El Ahmadieh TY, Plitt A, Kafka B et al (2019) H3 K27M mutations in thalamic pilocytic astrocytomas with anaplasia. World Neurosurg S1878–8750:30015–30014

70. Rodriguez FJ, Brosnan-Cashman JA, Allen SJ et al (2019) Alternative lengthening of telomeres, ATRX loss and H3–K27M mutations in histologically defined pilocytic astrocytoma with anaplasia. Brain Pathol 29:126–140

71. Ebrahimi A, Skardelly M, Schuhmann MU et al (2019) High frequency of H3 K27M mutations in adult midline gliomas. J Cancer Res Clin Oncol 4:839–850

72. Reers S, Krug D, Stummer W, Hasselblatt M (2017) Malignant progression of a histone H3.3 K27M-mutated spinal pilocytic astrocytoma in an adult. Clin Neuropathol 36:83–85

73. Louis DN, Giannini C, Capper D et al (2018) cIMPACT-NOW update 2: diagnostic clarifications for diffuse midline glioma, H3 K27M-mutant and diffuse astrocytoma/anaplastic astrocytoma, IDH-mutant. Acta Neuropathol 135:639–642

74. Pratt D, Natarajan SK, Banda A et al (2018) Circumscribed/non-diffuse histology confers a better prognosis in H3K27M-mutant gliomas. Acta Neuropathol 135:299–301

75. Fakhreddine MH, Mahajan A, Penas-Prado M et al (2013) Treatment, prognostic factors, and outcomes in spinal cord astrocytomas. Neuro Oncol 15:406–412

76. Reinhardt A, Stichel D, Schrimpf D et al (2018) Anaplastic astrocytoma with piloid features, a novel molecular class of IDH wildtype glioma with recurrent MAPK pathway, CDKN2A/B and ATRX alterations. Acta Neuropathol 136:273–291